

- C. A. Karlovich, C. Dasgupta, U. Banerjee, *ibid.* **255**, 603 (1992).
12. J. Brojatsh, J. Nanghton, M. M. Rolls, K. Zingler, J. A. Young, *Cell* **87**, 1 (1996).
13. W. C. Earnshaw, *Curr. Opin. Cell Biol.* **7**, 337 (1995).
14. C. Vincenz and V. M. Dixit, *J. Biol. Chem.* **272**, 6578 (1997).
15. Northern (RNA) blot analysis was performed with multiple tissue blots (Clontech, Palo Alto, CA) according to the manufacturer's instructions.
16. DR5, DR5Δ (amino acids 52 to 411), and TRID were cloned into pCMV1FLAG vector (IBI, Kodak). cDNAs encoding the extracellular domains of DR5 (amino acids 52 to 180) and TRID (amino acids 24

- to 163) were obtained by polymerase chain reaction and cloned into a modified pCMV1FLAG vector that allowed for in-frame fusion with the Fc portion of human IgG. The constructs expressing DR4, soluble TRAIL, and TNF-α have been described (4).
17. Cell death assays were done as described (5). MCF7 and HeLa cells were transfected with the lipofectamine procedure (BRL, Grand Island, NY), according to the manufacturer's instructions. 293 cells and 293T cells were transfected with calcium phosphate precipitation.
18. In vivo interaction assays have been described elsewhere (3).

19. The preparation of receptor-Fc fusions and ligands and in vitro binding assays has been described (4).
20. We thank A. M. Chinnaiyan, D. Chaudhary, H. Duan, S. Hu, E. Humke, K. Luetke, J. McCarthy, M. Muzio, H.-N. Nguyen, K. O'Rourke, Q. Song, and C. Vincenz for useful discussions and reagents; Y. Kuang for technical help; I. Jones for preparing figures; and J. DeJohn for secretarial assistance. Supported by NIH grants ES08111 and DAMD17-96-1-6085.

10 June 1997; accepted 10 July 1997

## Control of TRAIL-Induced Apoptosis by a Family of Signaling and Decoy Receptors

James P. Sheridan,\* Scot A. Marsters,\* Robert M. Pitti,\* Austin Gurney, Maya Skubatch, Daryl Baldwin, Lakshmi Ramakrishnan, Christa L. Gray, Kevin Baker, William I. Wood, Audrey D. Goddard, Paul Godowski, Avi Ashkenazi†

TRAIL (also called Apo2L) belongs to the tumor necrosis factor family, activates rapid apoptosis in tumor cells, and binds to the death-signaling receptor DR4. Two additional TRAIL receptors were identified. The receptor designated death receptor 5 (DR5) contained a cytoplasmic death domain and induced apoptosis much like DR4. The receptor designated decoy receptor 1 (DcR1) displayed properties of a glycospholipid-anchored cell surface protein. DcR1 acted as a decoy receptor that inhibited TRAIL signaling. Thus, a cell surface mechanism exists for the regulation of cellular responsiveness to pro-apoptotic stimuli.

Apoptosis (programmed cell death) is crucial for the development and homeostasis of metazoans (1). The cell death program has three essential types of elements: activators, inhibitors, and effectors; in *Caenorhabditis elegans*, these components are encoded, respectively, by the *ced-4*, *ced-9*, and *ced-3* genes. The CD95 ligand (CD95L) and tumor necrosis factor (TNF) are important extracellular activators of apoptosis in the mammalian immune system (2). The cognate receptors for these cytokines, CD95 (also called Fas or Apo1) and TNFR1, contain cytoplasmic "death domains" that activate the cell's apoptotic machinery through interaction with the death domains of the adapter proteins FADD (also called MORT1) (3, 4) and TRADD (5). Upon activation by ligand, CD95 recruits FADD directly, whereas TNFR1 binds FADD indirectly, through TRADD. FADD in turn

activates the *ced-3*-related protease MACHα/FLICE (caspase 8), thereby initiating a series of caspase-dependent events that lead to cell death (6, 7).

The cytokine TRAIL, also called Apo2L (8, 9), is structurally related to CD95L and TNF; TRAIL activates rapid apoptosis in tumor cell lines, acting independently of CD95, TNFR1, or FADD (9, 10). A receptor for TRAIL, designated DR4, belongs to the TNFR gene superfamily, contains a cytoplasmic death domain, and activates apoptosis independently of FADD (11). DR4 exhibits several mRNA transcripts that are expressed in multiple human tissues, including peripheral blood leukocytes (PBLs) and spleen (11).

On the basis of an expressed sequence tag (EST) that showed homology to death domains (12), we isolated human cDNAs encoding an undescribed member of the TNFR family, which we designated death receptor 5 (DR5) (Fig. 1A). The predicted DR5 precursor is a 411-amino acid type I transmembrane protein. DR5 shows more sequence identity to DR4 (55%) than to other apoptosis-linked receptors, namely, DR3 (also called Apo3, WSL-1, or TRAMP) (13–16) (29%), TNFR1 (19%), or CD95 (17%). DR5 and DR4 each con-

tain two extracellular cysteine-rich domains (CRDs) (Fig. 1A), whereas other mammalian TNFR family members have three or more CRDs (17). DR5 contains a cytoplasmic death domain that shows substantially more identity to the death domain of DR4 (64%) than to the death domain of DR3 (29%), TNFR1 (30%), or CD95 (19%).

Using a signal sequence trap approach and extracellular domain (ECD) homology (18, 19), we isolated an additional TNFR family member, which we named decoy receptor 1 (DcR1) (Fig. 1A). The DcR1 precursor is 259 amino acids long. DcR1 has a hydrophobic NH<sub>2</sub>-terminal sequence, followed by two CRDs. Downstream of the CRDs are five nearly identical tandem repeats, each 15 amino acids long; these repeats are followed by a hydrophobic COOH-terminus without an apparent cytoplasmic tail (Fig. 1A). This latter feature, together with the presence of a pair of small amino acids (Ala<sup>223</sup> and Ala<sup>224</sup>) just upstream of the hydrophobic COOH-terminus, suggests that DcR1 may be processed into a glycosyl-phosphatidylinositol (GPI)-anchored cell surface protein (20). The ECD of DcR1 is most closely related to those of DR4 (60% identity) and DR5 (50% identity) and contains five potential N-linked glycosylation sites (Fig. 1A).

We investigated the mRNA expression of DR5 and DcR1 in human tissues and tumor cell lines (Fig. 1B). We detected a single DR5 mRNA transcript and several DcR1 transcripts in multiple tissues; the ~1.5-kb DcR1 transcript corresponded in size to the cloned DcR1 cDNA. DR5 expression was relatively high in fetal liver and lung, and in adult PBL, ovary, spleen, liver, and lung. DcR1 expression was highest in PBL, spleen, lung, and placenta. Most of the tumor cell lines expressed DR5, but showed little or no expression of DcR1.

The sequence similarities between DR5, DcR1, and DR4 suggested that these receptors may interact with a common ligand. Epitope-tagged fusion proteins based on the ECD of DR5 or DcR1 (21) each coprecipitated with soluble TRAIL (22) (Fig. 2A). Other cytotoxic TNF family members, namely, TNF, lymphotoxin-α, or CD95L,

J. P. Sheridan, S. A. Marsters, R. M. Pitti, M. Skubatch, A. Ashkenazi, Department of Molecular Oncology, Genentech, South San Francisco, CA 94080–4918, USA.  
A. Gurney, D. Baldwin, L. Ramakrishnan, C. L. Gray, K. Baker, W. I. Wood, A. D. Goddard, P. Godowski, Department of Molecular Biology, Genentech, South San Francisco, CA 94080–4918, USA.

\*These authors contributed equally to this work.

†To whom correspondence should be addressed. E-mail: aa@gene.com

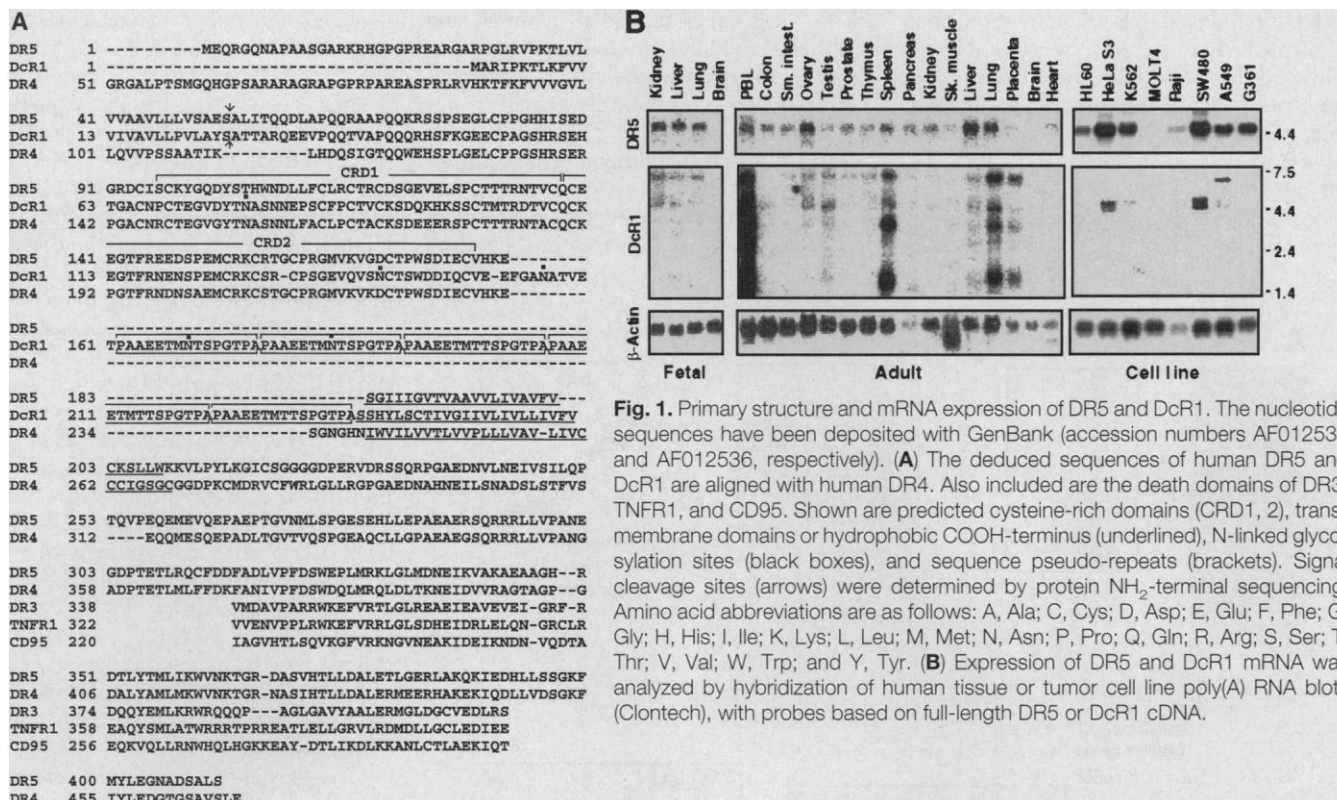


**Fig. 1.** Primary structure and mRNA expression of DR5 and DcR1. The nucleotide sequences have been deposited with GenBank (accession numbers AF012535 and AF012536, respectively). **(A)** The deduced sequences of human DR5 and DcR1 are aligned with human DR4. Also included are the death domains of DR3, TNFR1, and CD95. Shown are predicted cysteine-rich domains (CRD1, 2), transmembrane domains or hydrophobic COOH-terminus (underlined), N-linked glycosylation sites (black boxes), and sequence pseudo-repeats (brackets). Signal cleavage sites (arrows) were determined by protein NH<sub>2</sub>-terminal sequencing. Amino acid abbreviations are as follows: A, Ala; C, Cys; D, Asp; E, Glu; F, Phe; G, Gly; H, His; I, Ile; K, Lys; L, Leu; M, Met; N, Asn; P, Pro; Q, Gln; R, Arg; S, Ser; T, Thr; V, Val; W, Trp; and Y, Tyr. **(B)** Expression of DR5 and DcR1 mRNA was analyzed by hybridization of human tissue or tumor cell line poly(A) RNA blots (Clontech), with probes based on full-length DR5 or DcR1 cDNA.

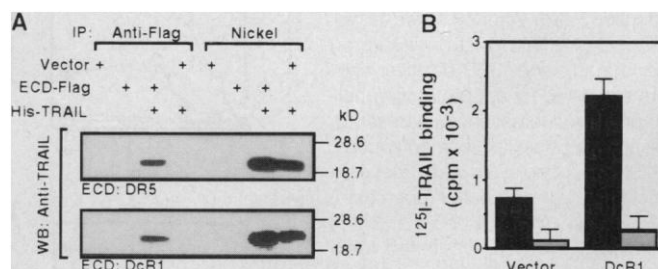
did not bind the DR5 or DcR1 ECDs (23). Thus, DR5 and DcR1 associate specifically with TRAIL.

To test whether DcR1 is GPI-linked, we analyzed the effect of recombinant phosphatidylinositol-specific phospholipase C (PI-PLC) (24) on the binding of TRAIL to intact DcR1-transfected cells (Fig. 2B). Transfection of human 293 cells by DcR1 led to an increase in the amount of specific TRAIL binding, consistent with interaction between DcR1 and TRAIL. DcR1 was not detected in the supernatants of DcR1-transfected cells (25), indicating that the protein is not secreted into the medium. Treatment by PI-PLC caused a marked reduction in TRAIL binding to cells (Fig. 2B), supporting the notion that DcR1 is GPI-anchored. This conclusion was substantiated by a 58% reduction in epitope tag-directed immunofluorescent staining of cells transfected with epitope-tagged DcR1 after PI-PLC treatment (26).

Because death domains function as oligomerization interfaces, overexpression of receptors that contain such domains leads to activation of signaling in the absence of ligand (2). To investigate whether DR5 can induce cell death, we transfected 293 or HeLa cells with a DR5 expression plasmid and assessed the level of apoptosis after 24 hours. DR5-transfected cells underwent apoptosis, as indicated by morphological changes, internucleosomal DNA fragmentation, and exposure of phosphatidylserine on the cell surface (Fig. 3,

A to C). The caspase inhibitors CrmA, DEVD-fmk, and z-VAD-fmk blocked apoptosis activation by DR5, indicating caspase involvement in this response. A dominant-negative form of the adapter FADD (FADD-DN), which blocks apoptosis induction by CD95, TNFR1, or DR3 (5, 13, 27) but not by TRAIL (10) or DR4 (11), did not inhibit apoptosis induction by DR5 (Fig. 3C), indicating that DR5 signals apoptosis independently of FADD. Consistent with previous work (10), TRAIL induced apoptosis in HeLa cells, which was blocked by immunoglobulin-fusion proteins (immunoadhesins) (28–30)

**Fig. 2.** **(A)** Interaction of DR5 and DcR1 with TRAIL. Supernatants from pRK5 vector-transfected 293 cells or from cells transfected by pRK5 encoding FLAG epitope-tagged DR5 or DcR1 ECD (5 ml) (21) were incubated with 1 μg of soluble, poly(His)-tagged TRAIL (22) for 30 min at 24°C. Complex formation with DR5 (top) or DcR1 (bottom) was tested by immunoprecipitation (IP) with anti-FLAG-conjugated (Sigma) or Ni-conjugated (Qiagen) agarose beads, followed by electrophoresis under reducing conditions and protein immunoblot (western blot, WB) with anti-TRAIL (34). **(B)** Effect of PI-PLC on the binding of TRAIL to DcR1-transfected cells. 293 cells were transiently transfected (35) by pRK5 vector or pRK5 encoding full-length DcR1. After 18 hours, the cells were put into suspension, treated with buffer (solid bars) or recombinant PI-PLC (1 μg/ml) (shaded bars) (24) for 2 hours at 37°C, and the binding of <sup>125</sup>I-TRAIL (0.2 ng) to intact cells (10<sup>6</sup> per tube) was analyzed. Nonspecific binding was measured in the presence of 500-fold excess unlabeled TRAIL. Data are the means ± SEM of triplicate determinations.



and DR3 induced NF- $\kappa$ B activation (Fig. 3E). Antibody to the p65 subunit of NF- $\kappa$ B inhibited the mobility of the NF- $\kappa$ B probe, implicating p65 in the response to all three receptors. TRAIL also induced detectable NF- $\kappa$ B activation in HeLa and 293 cells, but not in MCF7 cells (Fig. 3F); TNF induced a more pronounced activation in each cell line. Thus, TRAIL activates NF-

$\kappa$ B in a cell type-dependent manner, and both DR5 and DR4 can mediate this function. Dose-response analysis showed that TNF activates NF- $\kappa$ B at substantially lower concentrations than does TRAIL (25), suggesting distinct signaling mechanisms for NF- $\kappa$ B induction.

The absence of a cytoplasmic region in DcR1 suggested that this receptor is involved

in modulation, rather than in actual transduction, of TRAIL signaling. We investigated the effect of DcR1 expression on cellular responsiveness to TRAIL. Ectopic expression of DcR1 reduced sensitivity to apoptosis induction by TRAIL in 293 cells (Fig. 4A), as well as in HeLa cells (26). Six of the eight tumor cell lines that expressed little or no DcR1—HL-60, HeLa, MOLT-4, Raji, SW40, and A549 (Fig. 1B)—were sensitive to TRAIL-induced apoptosis (8–10, 26). In contrast, primary human umbilical vein endothelial cells (HUVEC), human microvascular endothelial cells (HUMEC), and PBLs, which expressed DcR1 (25) (Fig. 1B), were resistant to TRAIL (Fig. 4, C and D) (25). PI-PLC treatment of untransfected 293 cells sensitized these cells to apoptosis induction by TRAIL, but not by antibody to CD95 (anti-CD95) (Fig. 4B), consistent with removal of endogenous GPI-linked DcR1 from the cell surface. In addition, PI-PLC treatment of HUVEC or HUMEC sensitized these cells to TRAIL-induced apoptosis (Fig. 4, C and D). Hence, DcR1 inhibits TRAIL function, and DcR1 expression correlates with resistance to TRAIL.

The existence of multiple receptors for TRAIL suggests an unexpected complexity in the regulation of signaling by this cytokine. The two signaling receptors, DR4 and DR5, appear to be functionally redundant, and their expression patterns are not sufficiently different to suggest a distinct, tissue-specific involvement in TRAIL signaling. One possible explanation is that expression of DR4 and DR5 may differ at the level of individual cell types within tissues. The two receptors also may have additional, nonredundant signaling functions, perhaps mediated by regions outside the death domain.

TRAIL, DR4, and DR5 are expressed in multiple human tissues. The expression of a decoy receptor for TRAIL in normal tissues but not in many tumor cell lines suggests an explanation for the resistance of normal tissues and the broad sensitivity of tumor cell lines to TRAIL-induced apoptosis. Several TNFR superfamily members (for example, TNFR1 and TNFR2) are shed from the cell surface to form soluble inhibitors that neutralize their ligands at remote locations, for example, in the bloodstream (17). As a membrane-anchored protein, DcR1 can inhibit responsiveness to its ligand directly at the cell surface. Perhaps this mode of regulation represents a general mechanism that protects cells against the action of potent pro-apoptotic cytokines.

## REFERENCES AND NOTES

1. H. Steller, *Science* **267**, 1445 (1995).
2. S. Nagata, *Cell* **88**, 355 (1997).
3. M. Boldin *et al.*, *J. Biol. Chem.* **270**, 387 (1995).
4. A. M. Chinnaiyan, K. O'Rourke, M. Tewari, V. M. Dixit, *Cell* **81**, 505 (1995).

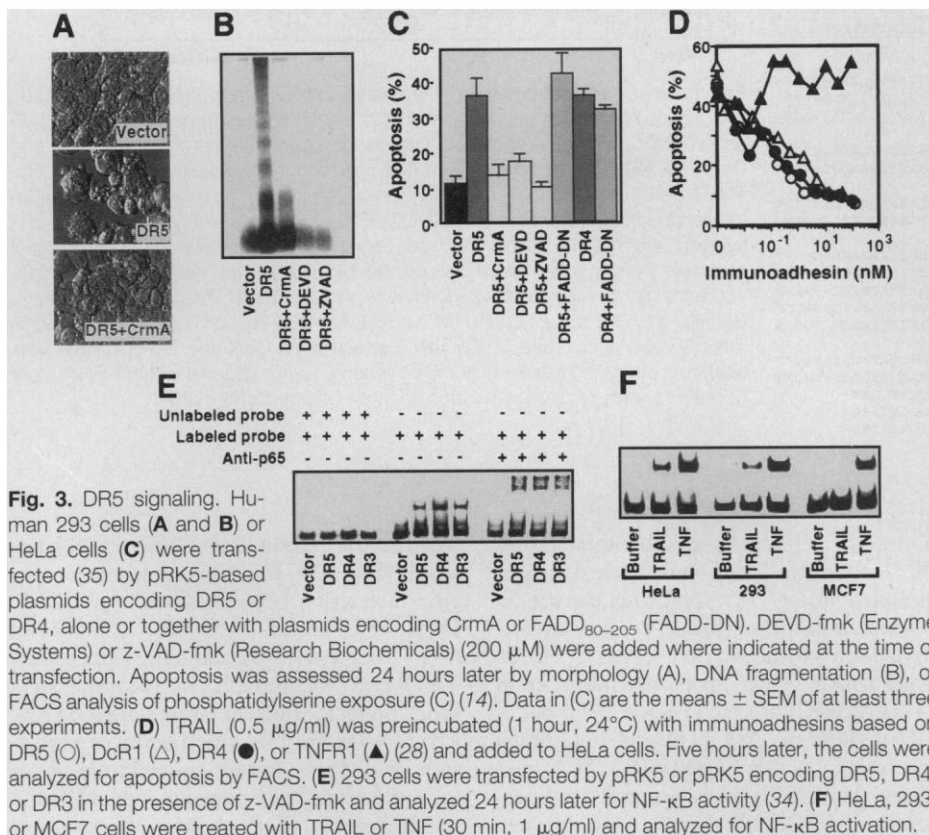


**Fig. 3.** DR5 signaling. Human 293 cells (A and B) or HeLa cells (C) were transfected (35) by pRK5-based plasmids encoding DR5 or DR4, alone or together with plasmids encoding CrmA or FADD<sub>80–205</sub> (FADD-DN), DEVD-fmk (Enzyme Systems) or z-VAD-fmk (Research Biochemicals) (200  $\mu$ M) were added where indicated at the time of transfection. Apoptosis was assessed 24 hours later by morphology (A), DNA fragmentation (B), or FACS analysis of phosphatidylserine exposure (C) (14). Data in (C) are the means  $\pm$  SEM of at least three experiments. (D) TRAIL (0.5  $\mu$ g/ml) was preincubated (1 hour, 24°C) with immunoadhesins based on DR5 (O), DcR1 ( $\Delta$ ), DR4 ( $\bullet$ ), or TNFR1 ( $\blacktriangle$ ) (28) and added to HeLa cells. Five hours later, the cells were analyzed for apoptosis by FACS. (E) 293 cells were transfected by pRK5 or pRK5 encoding DR5, DR4, or DR3 in the presence of z-VAD-fmk and analyzed 24 hours later for NF- $\kappa$ B activity (34). (F) HeLa, 293, or MCF7 cells were treated with TRAIL or TNF (30 min, 1  $\mu$ g/ml) and analyzed for NF- $\kappa$ B activation.

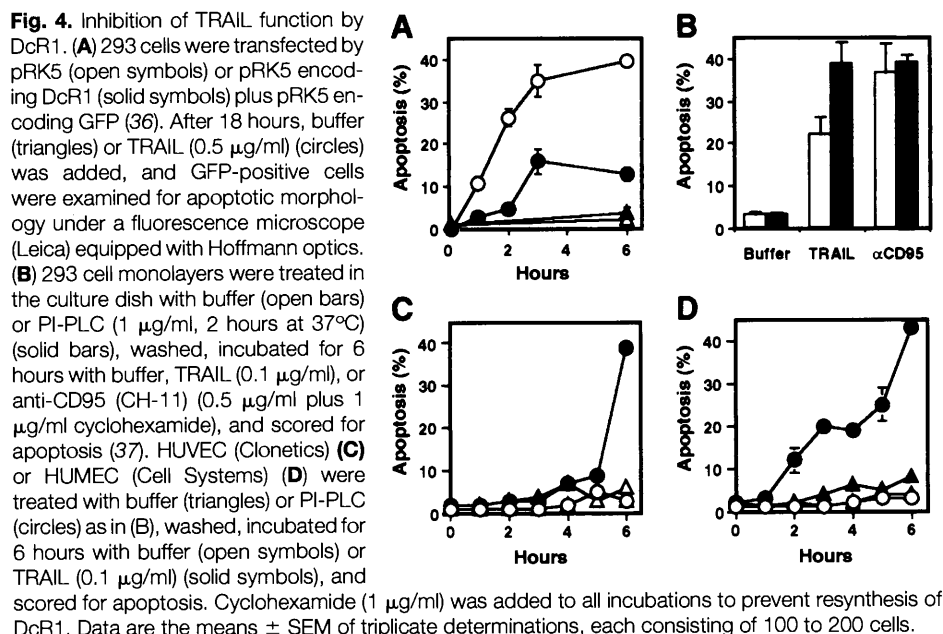


**Fig. 4.** Inhibition of TRAIL function by DcR1. (A) 293 cells were transfected by pRK5 (open symbols) or pRK5 encoding DcR1 (solid symbols) plus pRK5 encoding GFP (36). After 18 hours, buffer (triangles) or TRAIL (0.5  $\mu$ g/ml) (circles) was added, and GFP-positive cells were examined for apoptotic morphology under a fluorescence microscope (Leica) equipped with Hoffmann optics. (B) 293 cell monolayers were treated in the culture dish with buffer (open bars) or PI-PLC (1  $\mu$ g/ml, 2 hours at 37°C) (solid bars), washed, incubated for 6 hours with buffer, TRAIL (0.1  $\mu$ g/ml), or anti-CD95 (CH-11) (0.5  $\mu$ g/ml plus 1  $\mu$ g/ml cyclohexamide), and scored for apoptosis (37). HUVEC (Clonetics) (C) or HUMEC (Cell Systems) (D) were treated with buffer (triangles) or PI-PLC (circles) as in (B), washed, incubated for 6 hours with buffer (open symbols) or TRAIL (0.1  $\mu$ g/ml) (solid symbols), and scored for apoptosis. Cyclohexamide (1  $\mu$ g/ml) was added to all incubations to prevent resynthesis of DcR1. Data are the means  $\pm$  SEM of triplicate determinations, each consisting of 100 to 200 cells.

5. H. Hsu, H. B. Shu, M. G. Pan, D. V. Goeddel, *ibid.* **84**, 299 (1996).
6. M. Boldin, T. Goncharov, Y. Goltsev, D. Wallach, *ibid.* **85**, 803 (1996).
7. M. Muzio *et al.*, *ibid.*, p. 817.
8. S. R. Wiley *et al.*, *Immunity* **3**, 673 (1995).
9. R. M. Pitti *et al.*, *J. Biol. Chem.* **271**, 12697 (1996).
10. S. Marsters *et al.*, *Curr. Biol.* **6**, 750 (1996).
11. G. Pan *et al.*, *Science* **276**, 111 (1997).
12. On the basis of an EST from the Incyte Lifeseq Database that showed death domain homology, we designed a hybridization probe and used it to isolate the DR5 cDNA (Apo2, DNA27868) by screening human cDNA libraries. We isolated three cDNA clones encoding DR5: two from pancreas and one from kidney. The overlapping coding region was identical except for codon 410; this position encoded a leucine (TTG) in both pancreatic clones and a methionine (ATG) in the kidney clone.
13. A. M. Chinnaiyan *et al.*, *Science* **274**, 990 (1996).
14. S. Marsters *et al.*, *Curr. Biol.* **6**, 1669 (1996).
15. J. Kitson *et al.*, *Nature* **384**, 372 (1996).
16. J. L. Bodmer *et al.*, *Immunity* **6**, 79 (1997).
17. C. A. Smith, T. Farrah, R. G. Goodwin, *Cell* **76**, 959 (1994).
18. We identified the 5' region of DcR1 initially by sequence homology with TNFR1, from a collection of secreted proteins in a signal sequence trap analysis (19). Using a hybridization probe based on this sequence, we isolated cDNA clones encoding full-length DcR1 (Apo2DcR, DNA33085) by screening a human fetal lung library.
19. K. Baker and A. Gurney, unpublished data.
20. P. Moran, H. Raab, W. J. Kohr, I. W. Caras, *J. Biol. Chem.* **266**, 1250 (1991).
21. cDNA encoding the ECD of DR5 or DcR1 (amino acids 1 to 184 or 1 to 241, respectively) was amplified by polymerase chain reaction and fused at the COOH-terminus to a FLAG epitope tag (Sigma) within pRK5.
22. Soluble human TRAIL (Apo2L) was generated by fusing amino acids 114 to 281 to an NH<sub>2</sub>-terminal His<sub>10</sub> sequence, expression in *Escherichia coli*, and purification by Ni affinity chromatography as described (9). A different form of recombinant soluble TRAIL (amino acids 95 to 281) (8) has similar activity.
23. R. M. Pitti and A. Ashkenazi, unpublished data.
24. J. A. Koke, M. Yang, D. H. Henner, J. J. Volwerk, O. H. Griffith, *Protein Expr. Purif.* **2**, 51 (1991).
25. S. A. Marsters and A. Ashkenazi, unpublished data.
26. J. P. Sheridan and A. Ashkenazi, unpublished data.
27. A. M. Chinnaiyan *et al.*, *J. Biol. Chem.* **271**, 4961 (1996).
28. DR5 and DcR1 immunoadhesins were generated by fusing each receptor ECD to the hinge and Fc regions of human immunoglobulin G1 (IgG1) as described (29). DR4 and TNFR1 immunoadhesins were described previously (11, 30).
29. A. Ashkenazi and S. M. Chamow, *Methods: A Companion to Methods Enzymol.* **8**, 104 (1995).
30. A. Ashkenazi *et al.*, *Proc. Natl. Acad. Sci. U.S.A.* **88**, 10535 (1991).
31. L. A. Tartaglia, T. M. Ayers, G. H. W. Wong, D. V. Goeddel, *Cell* **74**, 845 (1993).
32. N. L. Malinin, M. P. Boldin, A. V. Kovalenko, D. Wallach, *Nature* **385**, 540 (1997).
33. A. Baldwin, *Annu. Rev. Immunol.* **14**, 649 (1996).
34. S. Marsters *et al.*, *J. Biol. Chem.* **272**, 14029 (1997).
35. Transient transfections were done by calcium phosphate precipitation (10 to 20  $\mu$ g of DNA per 10<sup>7</sup> cells) for 293 cells and by electroporation (10  $\mu$ g of DNA per 10<sup>6</sup> cells) for HeLa cells; in cotransfections, the total amount of plasmid DNA was kept constant with vector DNA.
36. Transient transfection of 293 cells by pRK5 itself resulted in sensitization to TRAIL-induced apoptosis relative to untransfected cells. The levels of background apoptosis in 293 cells as measured by morphology, directly in the culture dish (Fig. 4), were lower than the levels measured by fluorescence-activated cell sorting (FACS) analysis after harvest and staining of the cells with annexin V (9).
37. Treatment of 293 cell monolayers without removal from the culture dish led to a 33% reduction in <sup>125</sup>I-TRAIL binding (25), consistent with the 39% sensi-

zation to TRAIL-induced apoptosis of cells treated similarly with PI-PLC (Fig. 4B).

38. We thank C. Clark for comments; D. Goeddel for CrmA and FADD-DN plasmids; V. Dixit for DR4 and DR4-IgG plasmids; A. Rosenthal for PI-PLC; P. Juhani, P. Ng, and M. Vasser for DNA synthesis; J. Lee and A. Gray for cDNA libraries; C. Watanabe for

sequence analysis; M. Hamner for DNA sequencing; J. Tropea and W. Henzel for protein sequencing; S. Leung, J. Swartz, C. Blackie, and R. Pai for generating TRAIL; and the Genentech signal sequence trap team for help in cloning and expression.

4 June 1997; accepted 10 July 1997

## Neural Correlates of Motor Memory Consolidation

Reza Shadmehr\* and Henry H. Holcomb

Computational studies suggest that acquisition of a motor skill involves learning an internal model of the dynamics of the task, which enables the brain to predict and compensate for mechanical behavior. During the hours that follow completion of practice, representation of the internal model gradually changes, becoming less fragile with respect to behavioral interference. Here, functional imaging of the brain demonstrates that within 6 hours after completion of practice, while performance remains unchanged, the brain engages new regions to perform the task; there is a shift from prefrontal regions of the cortex to the premotor, posterior parietal, and cerebellar cortex structures. This shift is specific to recall of an established motor skill and suggests that with the passage of time, there is a change in the neural representation of the internal model and that this change may underlie its increased functional stability.

As one practices a motor task, stiffness of the limbs decreases (1), movements become smoother (2), and the muscle activations reflect a reliance of the motor output on an internal model (IM) that anticipates the force requirements of the task (3, 4). In a computational framework, the IM for arm movements may be characterized, in part (5), as a map from a desired trajectory for the hand to a set of muscle torques (6). Because we routinely use our hands to interact with a diverse variety of objects and systems, we rely on visual and haptic properties of the task to act as cues that facilitate recall of an appropriate IM from motor memory (7). Attempting to pick up an empty bottle of milk that has been painted white readily illustrates the consequences of visually cued recall of an inappropriate IM.

A single session of practice with a novel mechanical system may lead to long-term storage of an IM in the brain (8). However, when practice ends, a functional property of the IM continues to develop. Within 5 hours, the recently acquired IM gradually becomes resistant to behavioral interference (8, 9), that is, it consolidates. Although the mechanisms of motor memory

consolidation are unknown, examples from other memory systems of the brain show that a change in the neural representation of memory may contribute to consolidation (10). There is also evidence that neural representation of motor function is dynamic (11) and that motor areas of the primate brain are differentially associated with the performance of either a new or well-practiced motor task (12). Here we ask whether with the passage of time, as the IM becomes less fragile, there is a change in the neural representation of its motor memory.

We used positron emission tomography (PET) to monitor changes in regional cerebral blood flow (rCBF), an indirect marker of neural activity, mainly around the synapses (13), as participants ( $n = 16$ ) learned an IM of a novel mechanical system (Fig. 1A). The dynamics of the novel system were represented as a force field and were produced by the torque motors of a robotic arm (6). The task was to make rapid reaching movements to a series of targets while holding the handle of the robot (14). Participants initially practiced the task with the robot motors turned off (300 targets, during which no rCBF measures were taken). They made accurate, straight movements, similar to that shown in Fig. 1B. In session 1, we acquired rCBF measures (15) as participants performed the task during two repetitions of four successive conditions: (i) during a null field condition in which the robot's motors were off (Fig. 1B); (ii) during a random field condition in which the robot produced a random, non-

R. Shadmehr, Department of Biomedical Engineering, School of Medicine, Johns Hopkins University, 720 Rutland Avenue, 419 Traylor, Baltimore, MD 21205-2195, USA. E-mail: reza@bme.jhu.edu  
H. H. Holcomb, Maryland Psychiatric Research Center, University of Maryland, Post Office Box 21247, Baltimore, MD 21228, USA, and Department of Radiology, Johns Hopkins University, Baltimore, MD, USA. E-mail: hholcomb@mprcwb.ab.umd.edu

\*To whom correspondence should be addressed.